

Spectroscopic Characterization of a High-Potential Lipo-Cupredoxin Found in *Streptomyces coelicolor*

Jonathan A. R. Worrall,[†] Michael C. Machczynski, Bart J. F. Keijsers, Giulia di Rocco, Stefano Ceola, Marcellus Ubbink, Erik Vijgenboom, and Gerard W. Canters*

Contribution from the Leiden Institute of Chemistry, Leiden University, Gorlaeus Laboratories, P.O. Box 9502, 2300 RA Leiden, The Netherlands

Received June 22, 2006; E-mail: canters@chem.leidenuniv.nl

Abstract: For many streptomycetes, a distinct dependence on the “bioavailability” of copper ions for their morphological development has been reported. Analysis of the *Streptomyces coelicolor* genome reveals a number of gene products encoding for putative copper-binding proteins. One of these appears as an unusual copper-binding protein with a lipoprotein signal sequence and a cupredoxin-like domain harboring a putative Type-1 copper-binding motif. Cloning of this gene from *S. coelicolor* and subsequent heterologous expression in *Escherichia coli* has allowed for a thorough spectroscopic interrogation of this putative copper-binding protein. Optical and electron paramagnetic resonance spectroscopies have confirmed the presence of a “classic” Type-1 copper site with the axial ligand to the copper a methionine. Paramagnetic NMR spectroscopy on both the native Cu(II) form and Co(II)-substituted protein has yielded active-site structural information, which on comparison with that of other cupredoxin active sites reveals metal–ligand interactions most similar to the “classic” Type-1 copper site found in the amicyanin family of cupredoxins. Despite this high structural similarity, the Cu(II)/(I) midpoint potential of the *S. coelicolor* protein is an unprecedented +605 mV vs normal hydrogen electrode at neutral pH (amicyanin ~+250 mV), with no active-site protonation of the N-terminal His ligand observed. Suggestions for the physiological role/function of this high-potential cupredoxin are discussed.

Introduction

The present study focuses on the identification, isolation, and spectroscopic characterization of an unusual Type-1 blue copper protein that has two remarkable features: a surprisingly high midpoint potential and a signal sequence coding for attachment to a membrane lipid. Type-1 blue copper proteins, also referred to as cupredoxins, carry a single Cu atom and are known to occur in the three domains of life, i.e., bacteria, eukaryota, and archaea. However, for the Gram-positive bacteria, the actinomycetes, no report of the presence of a cupredoxin has so far occurred.

Members of the genus *Streptomyces* play an important role in the decomposition of large biopolymers. Their life cycle on solid media echoes that of fungi and is characterized by three main stages: (1) the formation of branched vegetative mycelium, a filamentous dense network of cells; (2) the formation of aerial hyphae, which rise above the mycelium; and (3) reproduction by the formation of unicellular spores at the tips of the aerial hyphae. Copper plays a crucial role in the developmental program of many streptomycetes:^{1–4} the morphological dif-

ferentiation of *Streptomyces lividans* and *Streptomyces coelicolor* is fully inhibited by the absence and stimulated by the presence of copper in the agar media.²

Copper-containing proteins are capable of performing a variety of functions. These range from participation in electron-transfer and enzymatic reactions^{5–7} to involvement in copper trafficking and homeostasis.^{8–11} The multifarious functions are in part dictated by the active-site coordination geometry of the copper ion(s), with different amino acid-binding motifs representative of the class and function of the protein.^{7,12–14} Knowledge of these copper-binding motifs can be used to identify putative copper proteins from known genome databases. With this in mind and recognizing the importance of copper in

[†] Present address: Department of Biochemistry, University of Cambridge, Cambridge CB2 1GA, U.K.

(1) Dionigi, C. P.; Ahten, T. S.; Wartelle, L. H. *J. Indust. Microbiol.* **1996**, *17*, 84–88.
(2) Keijsers, B. J. F.; van Wezel, G. P.; Canters, G. W.; Kieser, T.; Vijgenboom, E. *J. Mol. Microbiol. Biotechnol.* **2000**, *2*, 565–574.
(3) Kieser, T.; Hopwood, D. A. *Methods Enzymol.* **1991**, *204*, 430–458.

(4) Ueda, K.; Tomaru, Y.; Endoh, K.; Beppu, T. *J. Antibiot.* **1997**, *50*, 693–695.
(5) Fontecave, M.; Pierre, J. L. *Coord. Chem. Rev.* **1998**, *170*, 125–140.
(6) Messerschmidt, A. *Struct. Bonding* **1998**, *90*, 38–68.
(7) Sykes, A. G. *Adv. Inorg. Chem.* **1991**, *36*, 377–408.
(8) Banci, L.; Rosato, A. *Acc. Chem. Res.* **2003**, *36*, 215–221.
(9) Bertinato, J.; L’Abbe, M. R. *J. Nutr. Biochem.* **2004**, *15*, 316–322.
(10) Harrison, M. D.; Jones, C. E.; Solioz, M.; Dameron, C. T. *Trends Biochem. Sci.* **2000**, *25*, 29–32.
(11) Huffman, D. L.; O’Halloran, T. V. *Annu. Rev. Biochem.* **2001**, *70*, 677–701.
(12) Solomon, E. I.; Baldwin, M. J.; Lowery, M. D. *Chem. Rev.* **1992**, *92*, 521–542.
(13) Solomon, E. I.; Sundaram, U. M.; Machonkin, T. E. *Chem. Rev.* **1996**, *96*, 2563–2605.
(14) Solomon, E. I.; Szilagyi, R. K.; George, S. D.; Basumallick, L. *Chem. Rev.* **2004**, *104*, 419–458.

streptomycetes physiology, an inventory of genes encoding putative copper proteins on the *S. coelicolor* chromosome¹⁵ has been undertaken. This has yielded a “blueprint” of putative copper proteins.¹⁶ For proof of their copper-binding properties and their role in the physiology of *S. coelicolor*, biochemical and genetics studies are required. So far, of the putative copper proteins identified in *S. coelicolor*, the biophysical and biochemical characterization of only a multi-copper oxidase representing a new family of laccases has been reported.¹⁷

Type-I copper sites possess unique spectroscopic properties in their cupric state as a consequence of their coordination geometry. This makes cupredoxins highly amenable to spectroscopic studies.¹⁸ In particular, the application of NMR spectroscopy has proven to be a fruitful technique to study the paramagnetic cupric and other paramagnetic metal-substituted forms of these proteins. Such studies have yielded active-site structure information for numerous members of the cupredoxin family,^{19–28} allowing an intriguing insight into the subtle differences which exist in the metal–ligand interplay between the different families. Other spectroscopic techniques, such as optical, magnetic circular dichroism, and electron paramagnetic resonance spectroscopy, along with electrochemical analysis, have all played a major role in the characterization of cupredoxin active sites. Such studies have led to the Type-I sites being classified as “classic” and “perturbed”,^{29,30} where “classic” sites are associated with a weak copper–axial ligand bonding interaction³⁰ and perturbed sites with a stronger interaction.³¹ Both sites can be distinguished spectroscopically.

Analysis of the *S. coelicolor* chromosome has revealed a gene, SCO7674, which potentially codes for a cupredoxin-like protein possessing an N-terminal signal sequence which is characteristic of prokaryotic lipoproteins. Isolation of this gene and subsequent characterization of the product using spectroscopic and electrochemical techniques confirms that *S. coelicolor* possesses a cupredoxin-like protein with a “classic” Type-I copper site and is most likely lipid-tethered to a membrane. We find also that the Cu(II)/(I) redox couple is the highest known for a cupredoxin with a “classic” Type-I site. The new cupredoxin protein from *S. coelicolor* has been named lipocyanin (Lpc). It is the purpose

of the present paper to report on the metal-site properties of Lpc and discuss its possible role in streptomycetes morphological development.

Materials and Methods

Identification of Putative Copper Proteins in *S. coelicolor*.

Representative members of each known category of copper protein, along with the common copper-binding/copper-associated amino acid motifs, were used to search the *S. coelicolor* genomic database.¹⁵ The copper-associated motifs included the common copper-binding sites (Types I, II III, and IV, CuA and CuB), the heavy metal-associated motif, the metallothionein motif, and the copper-fist domain.^{32–37} Potential copper proteins were analyzed by protein-BLAST analysis³⁸ and motif detection using Pfam.³⁹ The potential cellular location of the putative copper proteins was predicted using the software on the CBS prediction server: SignalP, detecting potential export signal peptides;⁴⁰ TMHMM, predicting transmembrane regions; and LipoP, predicting lipoproteins.⁴¹ The genomic environment (potential operon structure and gene clusters) of the putative copper proteins was analyzed using the *S. coelicolor* genome sequence database (<http://streptomyces.org.uk>), and the gene products of neighboring genes were subjected to BLAST analysis and protein-domain detection. Finally, conservation of the genomic environment was analyzed using the STRING search algorithm.⁴²

Cloning of the SCO7674 Gene. All primers used for polymerase chain reaction (PCR) were designed such that direct cloning in the target vector was possible as well as cloning in a vector with a standard multiple cloning site such as pTZ19R.⁴³ Restriction enzyme sites added to the primers are underlined, and the numbers refer to the numbering of the *S. coelicolor* genome sequence. PCR reactions were carried out with HotStarTaq DNA polymerase (Qiagen) in the presence of 5% dimethylsulfoxide. The SCO7674 gene designated *lpc*, including upstream (SCO7673) and downstream (SCO7675) sequences, was obtained by PCR with genomic DNA of *S. coelicolor* as template and with the primers AMIF2 (GCCGAATTCGCTCCCGACATGAGCTGAGCGCG, 8497219–8497242) and AMIR2 (CGCAAGCTTCCGCGCGGTGCCCGGGGCTC, 8498928–8498905). The PCR product was cloned in the *EcoRI* and *HindIII* sites of pTZ19R. Several clones were sequenced, and the plasmid containing the right sequence was designated pSCAM1. Using pSCAM1 as template and the primers AMIF3 (GCCGAATTCATATGCCGTTCCCGTCCCGACCGGTG, 8498017–8498041) and AMIR2, a DNA fragment was generated with an *NdeI* site on the ATG start codon of *lpc*. This fragment was cloned in pET20 (Novagen), generating the plasmid pSCAM4 with *lpc* under the control of the T7 promoter.

To obtain a plasmid expressing Lpc without its signal sequence and without the Cys residue involved in possible lipid binding, a DNA fragment was amplified with pSCAM1 as template and the primers AMIF4 (CGGGAATTCATATGTCCGACGGGGGAG-

(15) Bentley, S. D.; et al. *Nature (London)* **2002**, *417*, 141–147.

(16) Keijsers, B. J. F. Ph.D. Thesis, University of Leiden, The Netherlands, 2003.

(17) Machczynski, M. C.; Vijgenboom, E.; Samyn, B.; Canters, G. W. *Protein Sci.* **2004**, *13*, 2388–2397.

(18) Canters, G. W.; Gilardi, G. *FEBS Lett.* **1993**, *325*, 39–48.

(19) Bertini, I.; Ciurli, S.; Dikiy, A.; Gasanov, R.; Luchinat, C.; Martini, G.; Safarov, N. *J. Am. Chem. Soc.* **1999**, *121*, 2037–2046.

(20) Bertini, I.; Fernandez, C. O.; Karlsson, B. G.; Leckner, J.; Luchinat, C.; Malmstrom, B. G.; Nersissian, A. M.; Pierattelli, R.; Shipp, E.; Valentine, J. S.; Vila, A. J. *J. Am. Chem. Soc.* **2000**, *122*, 3701–3707.

(21) Dennison, C.; Kohzuma, T. *Inorg. Chem.* **1999**, *38*, 1491–1497.

(22) Dennison, C.; Harrison, M. D. *J. Am. Chem. Soc.* **2004**, *126*, 2481–2489.

(23) Donaire, A.; Jimenez, B.; Fernandez, C. O.; Pierattelli, R.; Niizeki, T.; Moratal, J. M.; Hall, J. F.; Kohzuma, T.; Hasnain, S. S.; Vila, A. J. *J. Am. Chem. Soc.* **2002**, *124*, 13698–13708.

(24) Fernandez, C. O.; Sannazzaro, A. I.; Vila, A. J. *Biochemistry* **1997**, *36*, 10566–10570.

(25) Kalverda, A. P.; Salgado, J.; Dennison, C.; Canters, G. W. *Biochemistry* **1996**, *35*, 3085–3092.

(26) Salgado, J.; Kroes, S. J.; Berg, A.; Moratal, J. M.; Canters, G. W. *J. Biol. Chem.* **1998**, *273*, 177–185.

(27) Vila, A. J.; Ramirez, B. E.; DiBilio, A. J.; Mizoguchi, T. J.; Richards, J. H.; Gray, H. B. *Inorg. Chem.* **1997**, *36*, 4567–4570.

(28) Sato, K.; Dennison, C. *Biochemistry* **2002**, *41*, 120–130.

(29) LaCroix, L. B.; Randall, D. W.; Nersissian, A. M.; Hoitink, C. W. G.; Canters, G. W.; Valentine, J. S.; Solomon, E. I. *J. Am. Chem. Soc.* **1998**, *120*, 9621–9631.

(30) Randall, D. W.; Gamelin, D. R.; LaCroix, L. B.; Solomon, E. I. *J. Biol. Inorg. Chem.* **2000**, *5*, 16–29.

(31) van Gastel, M.; Canters, G. W.; Krupka, H.; Messerschmidt, A.; de Waal, E. C.; Warmerdam, G. C. M.; Groenen, E. J. J. *J. Am. Chem. Soc.* **2000**, *122*, 2322–2328.

(32) Bull, P. C.; Cox, D. W. *Trends Genet.* **1994**, *10*, 246–252.

(33) Castresana, J.; Lubben, M.; Saraste, M.; Higgins, D. G. *EMBO J.* **1994**, *13*, 2516–2525.

(34) Jungmann, J.; Reins, H. A.; Lee, J. W.; Romeo, A.; Hassett, R.; Kosman, D.; Jentsch, S. *EMBO J.* **1993**, *12*, 5051–5056.

(35) Ouzounis, C.; Sander, C. *FEBS Lett.* **1991**, *279*, 73–78.

(36) Messerschmidt, A.; Huber, R. *Eur. J. Biochem.* **1990**, *187*, 341–352.

(37) Southan, C.; Kruse, L. I. *FEBS Lett.* **1989**, *255*, 116–120.

(38) Altschul, S. F.; Gish, W.; Miller, W.; Myers, E. W.; Lipman, D. J. *J. Mol. Biol.* **1990**, *215*, 403–410.

(39) Bateman, A.; Birney, E.; Cerruti, L.; Durbin, R.; Ewinger, L.; Eddy, S. R.; Griffiths-Jones, S.; Howe, K. L.; Marshall, M.; Sonnhammer, E. L. L. *Nucleic Acids Res.* **2002**, *30*, 276–280.

(40) Bendtsen, J. D.; Nielsen, H.; von Heijne, G.; Brunak, S. *J. Mol. Biol.* **2004**, *340*, 783–795.

(41) Juncker, A. S.; Willenbrock, H.; von Heijne, G.; Brunak, S.; Nielsen, H.; Krogh, A. *Protein Sci.* **2003**, *12*, 1652–1662.

(42) Snel, B.; Lehmann, G.; Bork, P.; Huynen, M. A. *Nucleic Acids Res.* **2000**, *28*, 3442–3444.

(43) Mead, D. A.; Szczesna-Skorupa, E.; Kemper, B. *Protein Eng.* **1986**, *1*, 67–74.

CGGGTGGCGGC, 8498098–8498121) and AMIR3 (CGCAAGCT-TGGCAGGTCTCCGTTCGCGGCCG, 8498457–8498433). Following digestion with the restriction enzymes *Nde*I and *Hind*III, this fragment was ligated in pET28 (Novagen) digested with the same enzymes. The plasmid obtained, pSCAM17, expressed the truncated Lpc with an N-terminal His tag.

Recombinant Expression and Purification of Lpc. *Escherichia coli* BL21 (DE3) cells were transformed with pSCAM17, and single transformants were transferred to 30 mL of 2xYT medium containing 50 $\mu\text{g L}^{-1}$ kanamycin (Kan) and incubated overnight at 37°C. Two-liter Erlenmeyer flasks containing 750 mL of 2xYT medium, 50 $\mu\text{g L}^{-1}$ Kan, and 100 μM $\text{Cu}(\text{NO}_3)_2$ were inoculated with 5 mL of culture overnight and incubated at 30 °C until an OD_{600} of 1.5 was reached. At that point the temperature was reduced to 25 °C, and expression was induced with 500 μM isopropyl β -D-thiogalactopyranoside (IPTG). Incubation continued for a further 16 h, followed by centrifugation and resuspension of the cells in lysis buffer (20 mM tris(hydroxymethyl)methylamine (Tris)/HCl, pH 8, 500 mM NaCl, and 0.5 mM lysozyme). To this cell suspension were added 100 μM $\text{Cu}(\text{NO}_3)_2$, 150 μg of DNase I, and 10 μg of RNase, and lysis was achieved by passing the solution twice through a French press (1200 psi). (Adding a copper supplement before cell lysis helps to prevent uptake of other metals (e.g., zinc) after lysis.). The soluble fraction was collected by ultracentrifugation and batch-bound to Ni-NTA resin pre-equilibrated in 20 mM sodium phosphate, pH 8, and 5 mM imidazole. The N-terminal His₆-tagged Lpc eluted as a single peak in the presence of the equilibration buffer containing 500 mM imidazole and 300 mM NaCl. Fractions from the single peak were pooled and immediately dialyzed against 20 mM Tris/HCl, pH 8, and 150 mM NaCl to remove excess imidazole before removal of the His₆ tag by addition of thrombin (a total of 20 units). Dialysis continued with two changes of buffer. A final purification step, using a G-75 gel filtration column (Pharmacia) attached to an ÄKTA basic FPLC setup, resulted in a single major peak on the chromatogram. Fractions from this peak gave a single band on both sodium dodecyl sulfate–polyacrylamide gel electrophoresis (SDS–PAGE) and isoelectric focusing (IEF) gels.

Protein Samples for UV–Vis and Electrochemistry Measurements. Protein samples were fully oxidized using a solution of potassium hexachloroiridate(IV) (K_2IrCl_6) (Aldrich). Excess oxidant was removed using Centricon-10 units (Millipore). Stock solutions of Lpc were diluted in a mixed-buffer system consisting of 20 mM each 2-[*N*-cyclohexylamino]ethanesulfonic acid (CHES), *N*-[2-hydroxyethyl]piperazine-*N'*-[2-ethanesulfonic acid] (HEPES), and 2-[*N*-morpholino]ethanesulfonic acid (MES) and 50 mM sodium acetate. The pH of each sample was adjusted accordingly by addition of microliter aliquots of concentrated HCl or NaOH. Protein concentrations were typically 200 μM for electrochemical experiments and 50 μM for UV–vis measurements. The latter were performed on a Perkin-Elmer λ -800 spectrophotometer.

Electrochemical Measurements. Cyclic voltammetry (CV) studies were performed under argon using the electrochemical cell described by Hagen.⁴⁴ Measurements were made at 295 K with scan rates between 10 and 100 mV s⁻¹ using an Autolab potentiostat interfaced to a personal computer with GPES 4.3 software (Eco-Chemie, The Netherlands). A pyrolytic graphite electrode (PGE) was used as the working electrode, a saturated calomel electrode (SCE) as the reference electrode, and a Pt wire as the counter electrode. The SCE was calibrated with quinhydrone (Sigma) at 295 K. Prior to measurements, the PGE was polished with an Al₂O₃ (0.3 μm particle size) slurry on a Buehler polishing cloth, followed by a brief period (~1 min) of sonication in filtered water (Millipore). No further modification of the PGE was necessary to elicit a single reversible voltammetric wave.

EPR Spectroscopy. Protein samples for EPR measurements were typically >2 mM in concentration and were prepared in 25 mM MES,

pH 6.5, with 25–30% glycerol. Samples were treated with a slight excess of K_2IrCl_6 to make sure that all the protein was in the oxidized form. Continuous-wave EPR measurements were carried out on an X-band Bruker Elexsys 680 spectrometer (Bruker Biospin, Rheinstetten, Germany) with spectra acquired at 40 K, using a standard rectangular cavity provided with a helium flow cryostat. The amplitude of the 100 kHz field modulation was 1.0 G, and the spectra were recorded using a microwave power of 0.02 mW at 9.47972 GHz. The field was calibrated using 2,2-diphenyl-1-picrylhydrazyl ($g = 2.0036$). Experimental spectra were simulated using the Bruker program WINEPR SimFonia, with the g_{zz} and A_{zz} directly measured from the spectrum.

Preparation of Co(II)-Substituted Lpc. Apo-Lpc was prepared by incubation of the oxidized protein with 100 mM KCN in 150 mM Tris/HCl, pH 8, at room temperature for ~1 h. This solution was then exchanged into 20 mM HEPES, pH 8, by ultrafiltration (Amicon, 5 kDa cutoff membrane), followed by incubation at room temperature in the presence of 100 mM CoCl_2 for >12 h. The purple solution was loaded to a 10 \times 2.5 cm pre-equilibrated (diethylamino)ethyl sepharose column (20 mM HEPES, pH 8) attached to a Bio-Rad Econo system and eluted with a linear NaCl gradient (0–250 mM). UV–vis spectroscopy was used to check for fractions containing Co(II)-Lpc, which were subsequently pooled and concentrated for NMR studies.

Preparation of Samples for NMR Experiments. Samples of Cu(II)-Lpc for ¹H NMR studies were exchanged into 25 mM MES, pH 6.0 (95:5 H₂O/D₂O), or 10 mM MES, pH 5.3 (95:5 H₂O/D₂O and 99.9% D₂O), using Centricon-10 units. Cu(I)-Lpc samples were prepared by reducing the Cu(II) protein with a stoichiometric amount of sodium dithionite, followed by exchange into 20 mM sodium phosphate (NaPi), pH 8.0 (99.9% D₂O). Co(II)-Lpc samples were prepared in 20 mM NaPi, pH 8.0 (95:5 H₂O/D₂O and 99.9% D₂O). The pH of all protein solutions was adjusted when required with concentrated HCl or NaOH. The pH values quoted for deuterated solutions are uncorrected for the deuterium isotope effect.

¹H NMR Spectroscopy. All NMR spectra were recorded on a Bruker Avance DMX600 operating at a proton frequency of 600.13 MHz. For the detection of fast-relaxing paramagnetic signals in Cu(II)- and Co(II)-Lpc samples, a 1D superWEFT pulse sequence ($d1-180^\circ-\tau-90^\circ-\text{Acq}$, where $d1$ is the relaxation delay and Acq is the acquisition time) was employed.⁴⁵ Different interpulse delays ($\tau = 5-50$ ms) were used to optimize the detection of the paramagnetic signals and to minimize the solvent H₂O or the residual HDO signal. All spectra were acquired with spectral widths ranging between 100 and 200 kHz, processed with 20–50 Hz of exponential line broadening as apodization, and baselined using Bruker-provided software. Spin–lattice (T_1) relaxation times of the hyperfine-shifted resonances of Co(II)-Lpc were determined at 308 K using an inversion recovery experiment,⁴⁶ incorporating a superWEFT sequence with a total effective relaxation delay ($d1 + \text{Acq}$) ranging from 20 to 300 ms, with τ varied between 12.5 μs and the total effective relaxation delay. An exponential fit of the plots of peak intensity versus τ for selected hyperfine-shifted peaks was performed in the program Origin (Microcal), yielding their T_1 values. Likewise, peak widths were determined by fitting the peak of interest to a Lorentzian function in the same program. 1D nuclear Overhauser effect (NOE) experiments on Co(II)-Lpc samples were performed by using a modified superWEFT sequence, irradiating the resonance of interest during τ with a selective decoupler pulse. Spectra were acquired by alternating on- and off-resonance saturation of the selected peak, with the off-resonance spectra subtracted from their on-resonance counterparts to produce the NOE difference spectrum.

1D ¹H NMR spectra of Cu(I)-Lpc were acquired at 298 K with presaturation of the residual HDO signal and a spectral width of 8 kHz. For the detection of singlets in the aromatic region of the spectrum, Carr–Purcell–Meiboom–Gill (CPMG) [$90^\circ-\tau-(180^\circ-2\tau)_n-180^\circ-\tau$] ($n =$

(45) Inubushi, T.; Becker, E. D. *J. Magn. Reson.* **1983**, *51*, 128–133.

(46) Vold, R. L.; Waugh, J. S.; Klein, M. P.; Phelps, D. E. *J. Chem. Phys.* **1968**, *48*, 3831

(44) Hagen, W. R. *Eur. J. Biochem.* **1989**, *182*, 523–530.

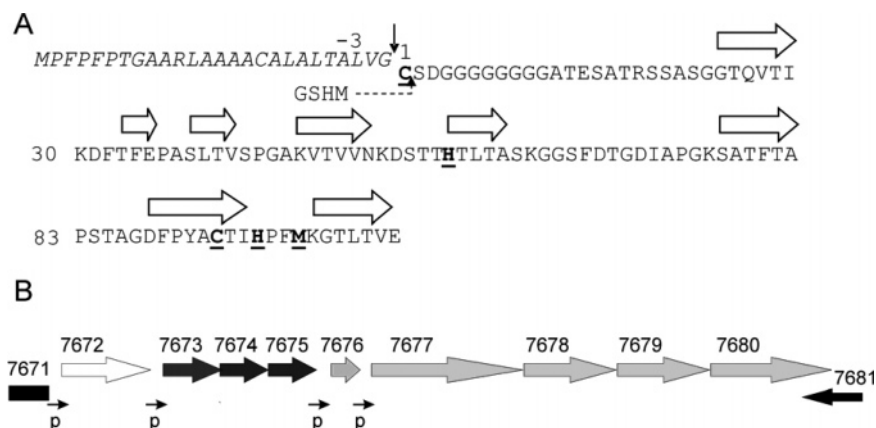


Figure 1. (A) Amino acid sequence of Lpc from *S. coelicolor*. The signal sequence is in italics, with the solid arrow indicating the putative signal peptidase II cleavage site and the Cys involved in likely attachment to a lipid shown in bold type. The dashed arrow indicates the additional four residues at the N-terminus for Lpc used in this work. The predicted ligands to the copper ion are in bold and are underlined, with the secondary structure prediction shown above the sequence.⁵² (B) The genomic environment of the *lpc* gene (SCO7674) with genes represented by block arrows and their SCO number (<http://streptomyces.org.uk>). SCO7671 and -7681 are transcribed in the opposite direction, and the genomic regions are found to contain consensus promoter sequences, as indicated with a P, with the direction of transcription indicated by the arrow. The intergenic spacing and the location of the putative promoters suggest that SCO7673 (lipoprotein), -7674 (Lpc), and -7675 (integral membrane protein with four transmembrane helices, TMH) are one transcription unit. This is also the case for SCO7677 (solute-binding (lipo)protein), -7678 (integral membrane protein with six TMH, putative ABC transporter), -7679 (integral membrane protein with six TMH, putative ABC transporter), and -7680 (ABC transporter, ATP-binding protein). SCO7672 is an integral membrane protein with six TMH, and SCO7676 is a ferredoxin. The number of TMH was analyzed using www.cbs.dtu.dk/services/TMHMM.

59, $\tau = 1$ ms) and Hahn spin-echo (HSE) [$90^\circ - \tau - 180^\circ - \tau$] ($\tau = 60$ ms) pulse sequences were used.⁴⁷ All chemical shifts are quoted with sodium 3-(trimethylsilyl)-*d*₄-propionate (TSP) as the internal reference.

Results

Identification of a Putative Cupredoxin-like Protein in *S. coelicolor*. Analysis of the 8.7 Mb linear genome of *S. coelicolor*¹⁵ using the copper-associated binding motifs identified 12 putative copper-containing proteins.¹⁶ The gene SCO7674 is identified to code for an extracellular protein that exhibits features characteristic of a cupredoxin and a signal peptide displaying properties of a bacterial lipoprotein. The primary sequence of this putative cupredoxin is shown in Figure 1A, with the amino acids at positions -3 to +1 (Leu-Val-Gly-Cys) displaying high similarity to the consensus sequence of a lipoprotein processing site.⁴⁸ The latter is proposed to be Leu-(Ala/Ser)-(Gly/Ala)-Cys, which is recognized by the signal peptidase II in bacteria.^{49,50} This enzyme cleaves the NH₂-terminal peptide bond of the Cys after it is modified by a thioether linkage to a diglyceride.⁵¹ Following on from this putative lipid anchor point, a stretch of eight Gly residues is present (Figure 1A), suggesting a highly flexible region of polypeptide tethering the remainder of the protein to the lipid. From the sequence-based fold prediction program GenTHREADER,⁵² a β -sandwich fold made up of eight β -strands interconnected by loops is predicted (Figure 1A). This fold is common to all cupredoxins with the C-terminal copper-binding motif, Cys-x-x-His-x-x-Met, indicating a Met as the axial copper ligand and an amino acid spacing between the potential copper ligands homologous to members of the amicyanin (Ami) family of cupredoxins. This analysis leads us to designate the gene (SCO7674) *lpc* and the product lipocyanin.

The neighboring gene environment of *lpc* indicates that the intergenic distance between the stop codon of the upstream ORF (SCO7673), encoding a lipoprotein, and the translation start of *lpc* is quite small (40 bp), with the translation stop codon of *lpc* overlapping with the start of a gene (SCO7675) encoding a transmembrane protein (Figure 1B). These genes may therefore form one operon. Further downstream, genes are found encoding a ferredoxin (SCO7676), a solute-binding protein (SCO7677), and a binding protein-dependent ABC transporter (SCO7678, -7679, and -7680), (Figure 1B).

Cloning and Recombinant Expression of Lpc. BL21 (DE3) transformed with pSCAM4 (*lpc* under control of the T7 promoter) did not produce a protein with the expected molecular weight, ~12 kDa, upon induction with IPTG, as judged from CBB-stained SDS-PAGE gels with whole cell lysates. This could be the result of incorrect processing of Lpc, as it contains the signal sequence and lipid attachment site of a Gram-positive bacterium. Therefore, a second expression plasmid was designed harboring the *lpc* gene, with the coding sequence for the signal peptide and the lipid attachment Cys deleted. Transformants with this plasmid were expected to produce the truncated form of Lpc in the cytoplasm. Following cell lysis, a heavy band at ~12 kDa appeared on an SDS-PAGE gel (not shown). Further purification (see Figure 2A) and subsequent removal of the N-terminal His₆ tag with thrombin resulted in a homogeneous product with a *pI* of 5.3 ± 0.2 and a mass of $10\,709 \pm 10$ Da, as determined by IEF and electrospray ionization mass spectrometry (ESI-MS), respectively. The mass corresponds to the apo-protein with sample preparation in acetonitrile and acetic acid and detection in the ESI-MS experiment using the positive ionization mode. In the absence of the N-terminal Cys, Lpc consists of 105 amino acids starting at Ser2. However, expression in pSCAM17 and removal of the His₆ tag results in a protein with an additional four residues (Gly-Ser-His-Met) at the N-terminus (Figure 1A) (see also Materials and Methods). Their presence is confirmed from the observed mass quoted above, which in the absence of copper is predicted to be

(47) Campbell, I. D.; Dobson, C. M.; Williams, R. J. P.; Wright, P. E. *FEBS Lett.* **1975**, *57*, 96-99.

(48) Hayashi, S.; Wu, H. C. *J. Bioenerg. Biomembr.* **1990**, *22*, 451-471.

(49) Inouye, S.; Franceschini, T.; Sato, M.; Itakura, K.; Inouye, M. *EMBO J.* **1983**, *2*, 87-91.

(50) Pollitt, S.; Inouye, S.; Inouye, M. *J. Biol. Chem.* **1986**, *261*, 1835-1837.

(51) Sankaran, K.; Wu, H. C. *J. Biol. Chem.* **1994**, *269*, 19701-19706.

(52) Jones, D. T. *J. Mol. Biol.* **1999**, *287*, 797-815.

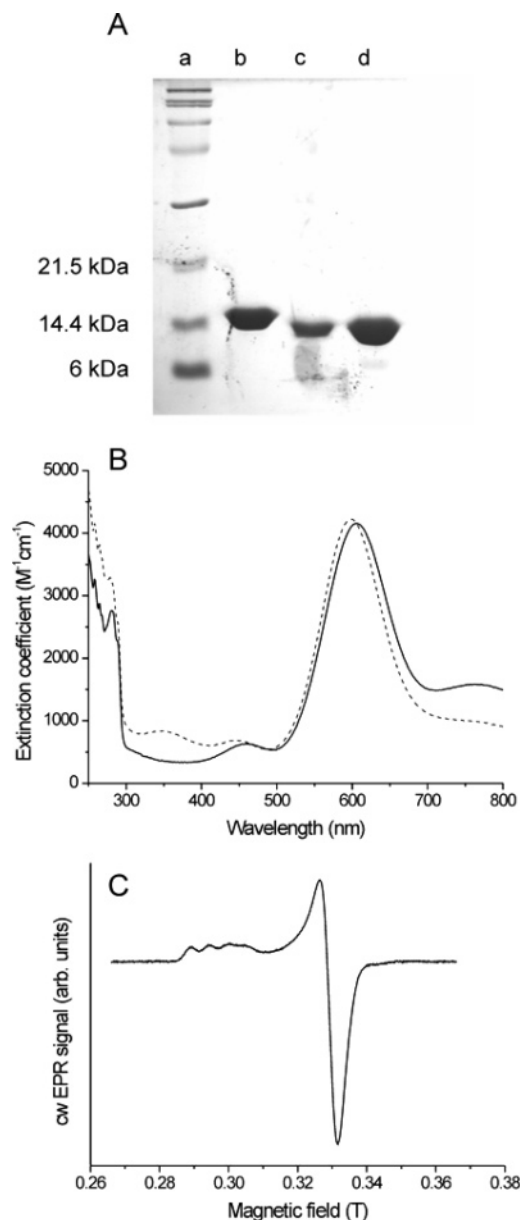


Figure 2. (A) SDS-PAGE gel of the recombinantly expressed Lpc stained with Coomassie blue. Lane a, molecular weight marker; lane b, after Ni-NTA column; lane c, after addition of thrombin, indicating removal of the His₆ tag; and lane d, after G-75 gel filtration chromatography. (B) UV-vis spectra at 295 K of Cu(II)-Lpc at pH 7.0 (solid) and pH 11.2 (dashed). (C) X-band EPR spectra at 40 K of Cu(II)-Lpc at pH 6.5.

10 703.7 Da. Typical yields of pure Lpc ranged between 25 and 50 mg L⁻¹, with the protein isolated and purified in its Cu(I) state (vide infra).

UV-Vis and EPR Spectroscopy of Lpc. Oxidation of Lpc was monitored by UV-vis spectrometry at pH 7.0. Addition of the oxidant K₃[Fe(CN)₆] after purification did not result in the typical blue color associated with an oxidized Cu(II) cupredoxin. This was only observed upon addition of the stronger oxidant, K₂[IrCl₆], resulting in the appearance of absorption bands at 460 and 606 nm in the optical spectrum (Figure 2B). These bands are assigned as transitions corresponding to one-electron excitations from mainly ligand-centered orbitals (S(Cys) pseudo- σ , Met, and His orbitals for the three transitions comprising the 450 nm band; Cys S(Cys)- π for the 606 nm band) to a copper-centered orbital with mainly d_{x²-y²}

character, in analogy with other cupredoxins.²⁹ Oxidation was considered to be complete when no further change in peak intensity at 460 and 606 nm occurred, resulting in an A_{460}/A_{606} ratio of 0.15. Incubation with Cu(NO₃)₂ resulted in no further spectral changes, indicating that the copper site was fully occupied. This was further confirmed by a bicinchoninic acid assay,⁵³ giving 1.3 ± 0.2 copper ions per Lpc molecule. The low absorbance at 280 nm compared with that of other cupredoxins is ascribed to the absence of a Trp residue in the Lpc sequence. In the pH range 4.0–9.5, the ligand-to-metal charge-transfer (LMCT) transitions are unchanged, but above pH 10, slight shifts are observed (Figure 2B). These coincide with an increase in the absorbance at 280 nm, a flattening of the very broad absorbance at 750 nm which is due to ligand field (LF) transitions, and the presence of a broad peak at ~350 nm (Figure 2B). No precipitation of the Cu(II) form of the protein was observed over the pH range studied, and the small changes observed at alkaline pH were completely reversible.

The X-band EPR spectrum of Cu(II)-Lpc is shown in Figure 2C. It is axial in appearance. Simulation of the spectrum generates the following parameters: $g_{xx} = 2.038$, $g_{yy} = 2.053$, $g_{zz} = 2.273$, and $A_{zz} = 52 \times 10^{-4}$ cm⁻¹. The axial g -tensor and the small hyperfine coupling constant (A_{zz}), along with the low A_{460}/A_{606} ratio observed by UV-vis spectroscopy, indicate that Lpc possesses a “classic” Type-1 copper site.^{29,30}

pH Dependence of the Midpoint Potential of Lpc. A single reversible voltammetric wave at 295 K and varying pH's was observed for Lpc using an unmodified PGE (Figure 3A). The peak separation in the CV experiments with scan rates ranging between 10 and 100 mV s⁻¹ was, on average, 58 mV, and the anodic and cathodic peak currents were almost identical and proportional to the square root of the scan rate (Figure 3A inset). Such behavior is consistent with a diffusion-controlled electrochemical process, with the average cathodic and anodic peak potentials taken as the E° of Lpc at the different pH values.⁵⁴

At pH 7, the E° for the Cu(II)/(I) equilibrium of Lpc is +605(3) mV versus normal hydrogen electrode. Compared to other cupredoxins with Met as the axial ligand, this value is larger by over 200 mV, with only the Cu(II)/(I) equilibrium of rusticyanin (Rc), +680 mV, being higher.^{55,56} Upon lowering of the pH, little variation in E° is observed (Figure 3B). Below pH 5, a slight increase occurs, with an E° of +627(4) mV at pH 3.1. For a number of cupredoxins, a considerable increase in E° is observed as the pH is lowered.⁵⁷ One such example is Ami, where the E° , as determined from protein film voltammetry,⁵⁸ increases from +230 to +375 mV between the pH's of 7 and 3, in agreement with CV data obtained from bulk solution studies.⁵⁴ The E° /pH profile has a slope of ~-55 mV/pH between pH's 6 and 4 (Figure 3B), consistent with the reduction of Cu(II)-Ami being accompanied by the uptake of a proton at the active site.⁵⁸ This active-site protonation (or acid transition) occurs at the solvent-exposed C-terminal His ligand, which becomes detached from the copper ion in the cuprous

(53) Brenner, A. J.; Harris, E. D. *Anal. Biochem.* **1995**, *226*, 80–84.

(54) Battistuzzi, G.; Borsari, M.; Canters, G. W.; de Waal, E.; Leonardi, A.; Ranieri, A.; Sola, M. *Biochemistry* **2002**, *41*, 14293–14298.

(55) Ingledew, W. J.; Cobley, J. G. *Biochim. Biophys. Acta* **1980**, *590*, 141–158.

(56) Lappin, A. G.; Lewis, C. A.; Ingledew, W. J. *Inorg. Chem.* **1985**, *24*, 1446–1450.

(57) Sykes, A. G. *Struct. Bonding (Berlin)* **1991**, *75*, 175–224.

(58) Jeuken, L. J. C.; Camba, R.; Armstrong, F. A.; Canters, G. W. *J. Biol. Inorg. Chem.* **2002**, *7*, 94–100.

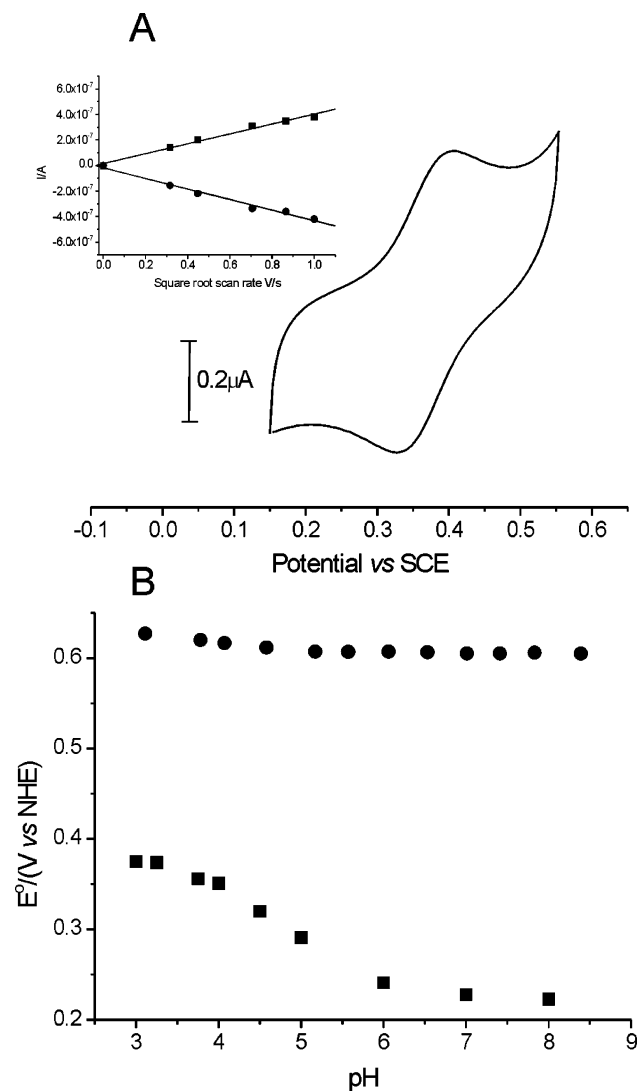


Figure 3. (A) CV of Lpc at 295 K and pH 7.0, using a PGE with a scan rate of 20 mV/s, starting in a reductive poise. The inset depicts a plot of the anodic (■) and cathodic (●) peak currents versus the square root of the scan rate. (B) pH dependence of the E° of Lpc at 295 K (●) along with Ami (■) for comparison. The latter was measured by protein film voltammetry with a PGE at 295 K.⁵⁸

state, resulting in an energetically more favored trigonal coordination geometry of the reduced copper site.⁵⁹ For Lpc, the E° /pH profile has a slope of ~ -10 mV/pH (Figure 3B), which is not consistent with an active-site protonation.

Effect of pH on the ^1H NMR Spectrum of Cu(I)-Lpc. The 1D ^1H NMR spectra of Cu(I) and Cu(II) Lpc gave well-resolved resonances in the aliphatic and amide regions, providing evidence that the *E. coli* purified protein was folded. For Cu(I)-Lpc, a combination of CPMG and HSE pulse sequences was used to discriminate among singlets, doublets, and triplets in the aromatic region of the spectrum at pH 7.5.⁴⁷ The singlets of the $C^{\epsilon 2}$ and $C^{\delta 2}$ protons of the imidazole rings are identified on the basis of their T_2 relaxation times, which are significantly longer than those for other aromatic protons. Two His residues (H57 and H96) are present in the amino acid sequence of Lpc, which are predicted to coordinate to the copper ion. Lpc, as coded by the pSCAM17 plasmid, contains a third His at -2 in

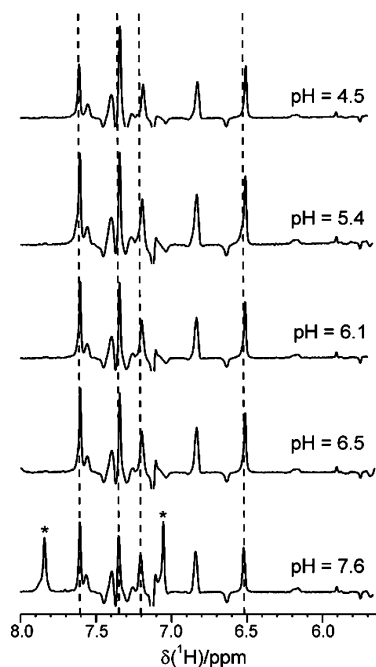


Figure 4. pH dependence of the Hahn spin-echo-derived ^1H NMR spectra of Cu(I)-Lpc at 298 K in D_2O . The six singlets arising from the nonexchangeable methylene imidazole protons of the three His residues in Lpc are indicated. The two peaks which disappear upon lowering the pH are marked with an asterisk, and the singlets belonging to the two copper-coordinating His residues are shown with dashed lines at different pH values. The peak at 6.82 ppm has not been assigned and possibly derives from a backbone amide proton.

the sequence (Figure 1A). This results in the detection of six singlets in the aromatic region of the Cu(I)-Lpc spectrum (Figure 4), which arise from the methylene protons of the imidazole rings. Specific assignments of these resonances to a particular His were not made in the present work. Upon decreasing the pH from 7.5, the singlets at 7.84 and 7.05 ppm disappear, whereas the remaining singlets at 7.61, 7.35, 7.21, and 6.51 ppm remain visible and exhibit very little change in their chemical shifts. The two singlets at 7.84 and 7.05 ppm are tentatively assigned to the His-2, as they are the only singlets present in the “diamagnetic region” of the spectrum of Cu(II)-Lpc. Their disappearance is probably connected with the pH-dependent proton-exchange equilibrium between the protonated and deprotonated forms of the imidazole side chain. The remaining singlets most likely arise from the two copper-coordinating His residues, with the absence of significant chemical shift changes with more acidic pH, consistent with the electrochemical data indicating that no active-site protonation of the copper-coordinating His residues occurs.

^1H NMR Spectrum of Cu(II)-Lpc. For Cu(II)-Lpc, the paramagnetic region of the ^1H NMR spectrum (Figure 5) shows a number of broad, hyperfine-shifted signals with chemical shifts which display a Curie-type temperature dependence (decrease in shift with increasing temperature, Figure 5A inset). Such temperature behavior has been reported for other Cu(II)-cupredoxins. The observed shifts (δ_{obs}) for a paramagnetic metalloprotein arise from three contributing factors, δ_{dia} , δ_{pc} , and δ_{Fc} , which together constitute the hyperfine shift. δ_{dia} is the shift in an analogous diamagnetic system, δ_{pc} is the pseudo-contact (through-space) contribution, and δ_{Fc} is the Fermi contact (through-bond) contribution. Due to the small anisotropy of the Cu(II)-cupredoxins g-tensor, the δ_{pc} is very small and the δ_{obs}

(59) Guss, J. M.; Harrowell, P. R.; Murata, M.; Norris, V. A.; Freeman, H. C. *J. Mol. Biol.* **1986**, *192*, 361–387.

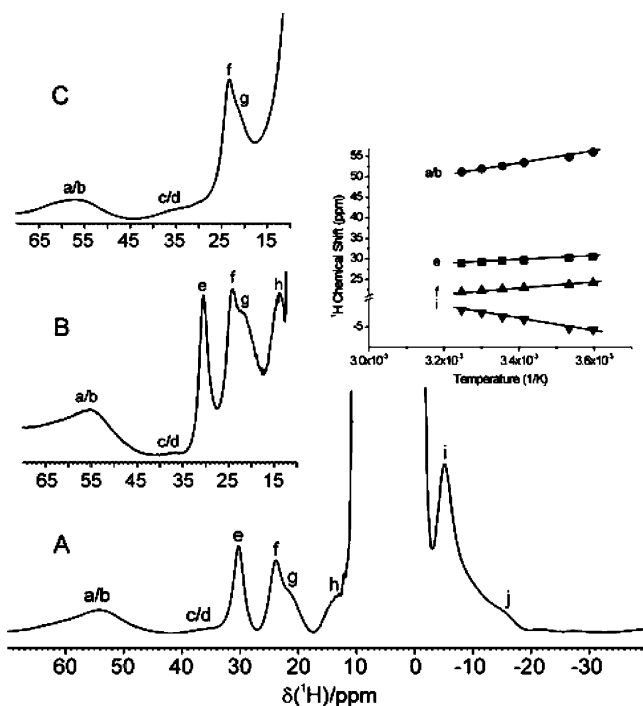


Figure 5. ^1H NMR spectra of Cu(II)-Lpc recorded at 600 MHz. (A) The spectrum at pH 5.3 and 283 K, with a plot of the effect on chemical shift for certain hyperfine-shifted signals with temperature at pH 6.0. (B) A section of the spectrum recorded at pH 6.0 and 278 K. (C) The spectrum recorded in D_2O at pH 5.3 and 283 K.

is therefore a reasonable indicator of the δ_{FC} , which is a measure of the spin density.

The broad resonances at ~ 54 (a/b) and ~ 36 ppm (c/d), the latter being more visible in the spectrum recorded in D_2O (Figure 5C), are assigned to the nonexchangeable imidazole ring protons of the coordinating His ligands. At 600 MHz, the spectral resolution is not sufficient to separate out individual peaks as reported at 800 MHz for other cupredoxins.^{19,20,23} Nevertheless, the positions of the active-site His signals vary little among cupredoxins, and the assignments made here for Cu(II)-Lpc are in analogy with previous findings (Table 1). The exchangeable signal e is assigned to the $\text{N}^{\epsilon}\text{H}$ of the copper ligand, His57, with no resonance observed for the corresponding proton of the His96 ligand. This is noted for other cupredoxins and arises from the latter proton being solvent-exposed and therefore in fast-exchange with bulk solvent. Attempts to slow this exchange by lowering the pH and temperature did not resolve another peak. In the upfield region of the spectrum, the sharp signal i likely arises from the C^{β}H of His57, whereas the broader signal j is most likely from the $\text{C}^{\alpha}\text{H}$ of the Cys93. Both signals display δ_{obs} values similar to those of other cupredoxins (Table 1).

For all cupredoxins, a relatively sharp signal with T_1 and T_2 relaxation times longer than those for the other hyperfine-shifted signals is observed between 14 and 20 ppm.¹⁹ This signal is assigned to the $\text{C}^{\alpha}\text{H}$ of the residue preceding the coordinating N-terminal His ligand and is often an Asn, although for Rc it is a Ser, and for members of the phycocyanins it is an Asp. However, regardless of residue type, a peak corresponding to the $\text{C}^{\alpha}\text{H}$ proton is always present. For Lpc, this residue is a Thr, and it is not immediately clear from the spectrum, contrary to other cupredoxin spectra, which is the corresponding signal. Signal f appears to be part of an overlapping set of peaks at ~ 23 ppm which, upon changing the pH and temperature,

becomes slightly better resolved (Figure 5B). The T_1 time of this peak is considerably higher than those of other signals in the paramagnetic region, and despite its more downfield chemical shift compared with other cupredoxins in Table 1, signal f is assigned to the $\text{C}^{\alpha}\text{H}$ of Thr58.

For plastocyanin (Pc) and Ami, the resonances corresponding to the $\text{C}^{\gamma}\text{H}_2$ protons of the axial Met ligand are observed outside of the diamagnetic envelope.^{19,25} For pseudoazurin (pAz) and Rc, these signals are absent.²³ For Ami and Pc, the differences in chemical shift for the $\text{C}^{\gamma}\text{H}$ assignments (Table 1) is suggested to arise from differences in the strength of the Cu–S(Met) interaction. For Lpc, the EPR and UV–vis data are consistent with a “classic” Type-1 copper site, and the $\text{C}^{\gamma}\text{H}$ resonances of the axial Met ligand would therefore be expected to be observed outside of the diamagnetic window. By simply comparing the Cu(II)-Lpc spectrum with those of Ami and Pc, it is not immediately obvious which signals may belong to the $\text{C}^{\gamma}\text{H}$ protons of the Met. However, as only two signals remain, g and h, both with chemical shifts similar to those observed in Pc, we have tentatively assigned these to the $\text{C}^{\gamma}\text{H}$ protons of Met99 (Table 1).

UV–Vis Spectrum and ^1H NMR Spectroscopy of Co(II)-Lpc. Substitution of the native Cu(II) ion in cupredoxins with a fast-relaxing paramagnetic metal ion such as Co(II) results in an NMR spectrum with well-resolved hyperfine-shifted resonances belonging to protons associated with the metal ion ligands. Such an approach is complementary to the paramagnetic NMR on the Cu(II) proteins, with Co(II)- and Ni(II)-substituted cupredoxins providing further active-site structural information.^{60–65} The main S(Cys) \rightarrow Co(II) LMCT occurs at 324 nm, and the LF transitions can be seen between 500 and 700 nm (Figure 6 inset). The low intensity of the latter is consistent with a distorted tetrahedral ligand geometry of the Co(II) ion.⁶⁴

The paramagnetic ^1H NMR spectrum of Co(II)-Lpc is similar in appearance to those of other Co(II)-cupredoxins, in particular Co(II)-Ami.⁶⁴ The active-site assignments of Co(II)-Lpc, along with their T_1 relaxation times and peak widths ($\Delta\nu_{1/2}$), are reported in Table 2. At pH 8.0 in D_2O , signal g is absent, with signal f being observed only at more acidic pH values in H_2O (Figure 6B). These observations are consistent with peaks f and g arising from the exchangeable $\text{N}^{\epsilon}\text{H}$ protons of the two His ligands. The appearance in the spectrum of peak f only at acidic pH's is indicative of the proton being solvent-exposed, leading to fast exchange with the bulk solvent at neutral pH and its absence in the spectrum. Signals f and g are therefore assigned to the $\text{N}^{\epsilon}\text{H}$ protons of copper ligands His96 and His57, respectively. Irradiation of peak g yielded an NOE to peak h, with the reciprocal dipolar connectivity obtained upon irradiation of peak h. Analysis of the line width and T_1 time of peak h (Table 2) indicates that this proton, in analogy with Co(II)-Ami, most likely belongs to the $\text{C}^{\delta}\text{H}$ of His96. Similarly, peak i is assigned to the $\text{C}^{\delta}\text{H}$ of His57. No dipolar connectivities could be detected for the broad signals d and j. The chemical

(60) Dennison, C.; Sato, K. *Inorg. Chem.* **2002**, *41*, 6662–6672.

(61) Dennison, C.; Sato, K. *Inorg. Chem.* **2004**, *43*, 1502–1510.

(62) Fernandez, C. O.; Niizeki, T.; Kohzuma, T.; Vila, A. J. *J. Biol. Inorg. Chem.* **2003**, *8*, 75–82.

(63) Salgado, J.; Jimenez, H. R.; Donaire, A.; Moratal, J. M. *Eur. J. Biochem.* **1995**, *231*, 358–369.

(64) Salgado, J.; Kalverda, A. P.; Diederix, R. E. M.; Canters, G. W.; Moratal, J. M.; Lawler, A. T.; Dennison, C. *J. Biol. Inorg. Chem.* **1999**, *4*, 457–467.

(65) Vila, A. J.; Fernandez, C. O. *J. Am. Chem. Soc.* **1996**, *118*, 7291–7298.

Table 1. Assignments of the Hyperfine-Shifted Signals Observed in the Paramagnetic Region of the NMR Spectrum of Cu(II)-Lpc, along with a Comparison of the Corresponding Protons of the Copper Ligands in Other Cu(II)-Cupredoxins with Met as the Axial Ligand^a

resonance	assignment ^a	δ_{obs} (ppm)					
		Lpc 283 K pH 6.0 600 MHz	Ami 308 K pH 7.0 600 MHz ^c	Pc 298 K pH 7.5 800 MHz ^e	Az 278 K pH 8.0 800 MHz ^f	pAz 298 K pH 8.0 800 MHz ^g	Rc 296 K pH 5.5 800 MHz ^g
a	HisC/N, C ^{β} H	~54.0	50.0 (C)	51.6 (C)	54.0 (C)	53.5 (C)	58.1 (C)
b	HisC/N, C ^{β} H	~54.0	43.0 (N)	47.1 (N)	49.1 (N)	46.1 (N)	50.2 (N)
c	HisC/N, C ^{ϵ} H	~36.0 ^b	<i>i</i>	35.6 (C/N)	46.7 (C/N)	32.0 (C/N)	36.7 (N)
d	HisC/N, C ^{ϵ} H	~36.0 ^b	<i>i</i>	35.6 (C/N)	34.1 (C/N)	32.0 (C/N)	30.3 (C)
e	HisN, N ^{ϵ} H	30.1	27.5	31.4	27.0	23.0	25.3
f	Thr58, C ^{α} H	23.8	14.1 ^d (Asn)	17.0 (Asn)	19.9 (Asn)	17.4 (Asn)	19.5 (Ser)
g	Met, C ^{γ} H	21.7	12.0 C ^{γ} H	23.5 C ^{γ} H	<i>i</i>	<i>i</i>	<i>i</i>
h	Met, C ^{γ} H	13.0	11.1 C ^{γ} H	13.0 C ^{γ} H	<i>i</i>	<i>i</i>	<i>i</i>
i	HisN, C ^{β} H	-5.1	-2.5	-1.5	-2.3	<i>j</i>	<i>j</i>
j	Cys, C ^{α} H	-15.4	-9.5	-8.0	-7.0	-8.7 ^h	-8.9
	Met, ϵ -CH ₃	<i>i</i>	<i>i</i>	<i>i</i>	<i>i</i>	12.1	8.1

^a C and N denote the C-terminal and the N-terminal His in the different cupredoxin species. ^b Detected at pH 5.3. ^c Ami from *Paracoccus versutus*.²⁵ ^d Reassigned in ref 19. ^e Pc from spinach.¹⁹ ^f Az from *Pseudomonas aeruginosa*.²⁰ ^g pAz from *Achromobacter cycloclastes* and Rc from *Thiobacillus ferrooxidans*.²³ ^h pAz from *A. cycloclastes*, pH 7.6, 323 K, 500 MHz.²⁸ ⁱ Not observed. ^j Chemical shift not reported.

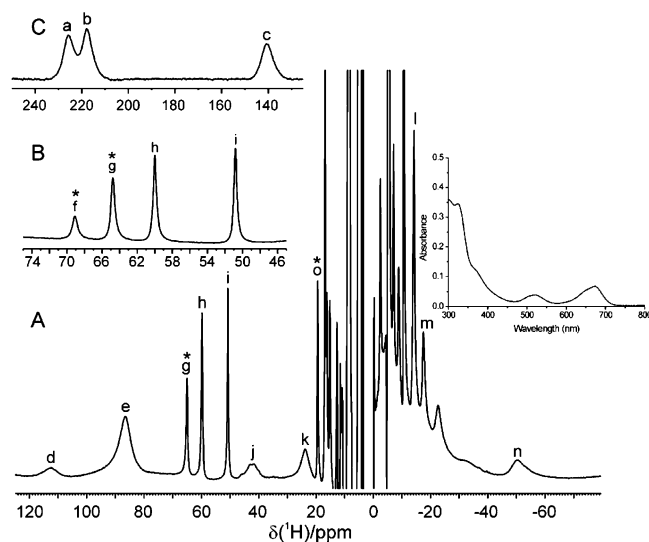


Figure 6. Paramagnetic ¹H NMR spectra of Co(II)-Lpc recorded in H₂O at 600 MHz and 308 K. (A) The 120 to -70 ppm region at pH 8.0, together with the UV-vis spectrum of Co(II)-Lpc at pH 8.0 and 295 K. (B) The 75 to 45 ppm region recorded at pH 4.9. (C) The 250–130 ppm region at pH 8.0. The asterisks indicate the peaks which are absent when the spectrum is recorded in D₂O.

shifts, T_1 times, and line widths (Table 2) are typical for C ^{ϵ} H protons of His coordinated to Co(II) via their N ^{δ} 1 atoms. Recently, Dennison and Sato⁶¹ have specifically assigned signal d in Co(II)-Pc to the C ^{ϵ} H proton of His87 (His96 in Lpc).

The large δ_{obs} displayed by signals a and b (Figure 6C) and the very short T_1 times (Table 2) are indicative of protons located only a few bonds away from the paramagnetic metal ion. In analogy with all other Co(II)-substituted cupredoxins, these signals are assigned to the C ^{β} H protons of the coordinating Cys93 ligand. Signal e has a peak area equivalent to three protons. It arises for the C ^{ϵ} H₃ group of the Met99 ligand. Irradiation of this peak does not result in a clear NOE to any other peak in the spectrum. This may be expected, given its short T_1 time and the distance between the C ^{ϵ} H₃ group and the other protons on a Met side chain. Signal c has a T_1 time and δ_{obs} (Table 2) very similar to those of the C ^{γ} H of the Met ligand in Co(II)-Ami⁶⁴ and is thus assigned to the analogous proton in Co(II)-Lpc. Irradiation of this signal does not yield any NOEs

Table 2. Assignments of the Hyperfine-Shifted Resonances of Co(II)-Lpc at 308 K and pH 8.0; Included for Comparison are the Chemical Shifts and Corresponding Assignments for Co(II)-Ami^b

resonance	δ_{obs} (ppm)	T_1 (ms)	$\Delta\nu_{1/2}$ (Hz)	assignment	δ_{obs} (ppm) for Ami ^b
a	225.6	n.d.	~3000	Cys93 C ^{β} H	~285
b	217.7	n.d.	~3000	Cys93 C ^{β} H	~285
c	140.4	~1.0	n.d.	Met99 C ^{γ} H	132.5
d	112.4	1.0 ± 0.2	~4000	His96/57 ^d C ^{ϵ} H	117.9
e	86.4	~1.0	2780	Met99 C ^{ϵ} H ₃	74.5
f	69.1 ^a	n.d.	n.d.	His57 N ^{ϵ} H	74.0 ^c
g	64.9	4.0 ± 0.1	340	His96 N ^{ϵ} H	62.3
h	59.8	20.3 ± 1.0	294	His57 C ^{δ} H	52.6
i	50.7	10.6 ± 0.5	266	His96 C ^{δ} H	51.0
j	42.3	~0.5	>3000	His96/57 C ^{ϵ} H	37.8
k	23.8	n.d.	1690	Met99 C ^{γ} H	10.0
l	-10.7	9.1 ± 1.8	156	Met99 C ^{β} H	-16.1
m	-14.2	3.4 ± 0.2	358	Met99 C ^{β} H	-18.6
n	-50.4	n.d.	n.d.	His96 C ^{β} H	n.d.

^a Data recorded at pH 4.9, 308 K. ^b Data recorded at pH 8.0, 313 K. ^c At pH 5.0, 295 K and taken from ref 64. ^d In *Paracoccus versutus* Ami, it is His54.

to other peaks. For signals l and m, the δ_{obs} and T_1 values are very similar to those of the C ^{β} H protons of the Met ligand in Co(II)-Ami (Table 2).⁶⁴ Furthermore, irradiation of signal l or m gives strong NOEs to each other, indicative of them belonging to geminal protons. Signal l displays a slightly longer T_1 time than signal m, which upon comparison with Co(II)-Ami⁶⁴ and Co(II)-Pc⁶¹ is consistent with signal l belonging to the C ^{β} H and m to the C ^{β} H of Met99.

For the remaining signals, only tentative assignments are made. From the T_1 time, line width, and similarity to signal c, signal k is assigned to the other C ^{γ} H proton of Met99. In Co(II)-Ami, a broad peak for this proton is observed at 10 ppm.⁶⁴ A subtle change in the metal–ligand interplay in Co(II)-Lpc may be a reason to shift this proton to a more downfield position. Signal n, the most upfield-shifted peak, has a δ_{obs} and line shape very similar to those of the resonance assigned to the C ^{β} H of His87 in Co(II)-Pc.⁶¹ Finally, signal o is also absent when the spectrum is recorded in D₂O. This suggests that signal o arises from an exchangeable proton, possibly belonging to a backbone amide in close proximity to the metal ion, which experiences a considerable hyperfine shift.

Discussion

Lpc is a Cupredoxin. Cloning of the full-length *lpc* gene into an *E. coli* vector resulted in no expression of a cupredoxin-like protein. However, spectroscopic features indicative of a Type-1 “blue” copper site were observed for the recombinant Lpc lacking the N-terminal Cys residue. From the EPR data, the hyperfine coupling constant ($A_z = 52 \times 10^{-4} \text{ cm}^{-1}$) is consistent with the axial ligand to the copper ion being a non-oxygen atom, with the relatively small differences between the g_x and g_y components along with the low absorbance at 460 nm in the UV–vis spectrum placing Lpc with the cupredoxins Pc, Ami, and azurin (Az), possessing an axial Met ligand and a “classic” Type-1 copper site.¹⁴

Comparison of the δ_{obs} values for the two His ligands and the C^αH proton of Cys93 with the other cupredoxins listed in Table 1 indicates a highly homologous spin density distribution over the active site in all these proteins. This is further illustrated by the presence of peak f in the spectrum, arising from the C^αH proton of Thr58, which experiences a large δ_{Fc} contribution due to its backbone amide H-bonding to the thiolate of the Cys93 ligand. This resonance is observed in all other cupredoxin spectra, regardless of the residue preceding the N-terminal His ligand. The significant δ_{obs} for these two C^αH protons suggests a significant spin density on the Cys93 ligand.

Further conformation for a “classic” Type-1 site comes from the presence of peaks g and h in the paramagnetic region of the spectrum, tentatively assigned to the C^γH protons of Met99. The positions of these peaks provide evidence for a Cu(II)–Met interaction similar in strength to the same reactions in Pc and Ami.^{19,25} The behavior of the exchangeable N^{ε2}H protons of the His ligands indicates a degree of active-site solvent accessibility similar to that seen for the cupredoxins listed in Table 1. Therefore, it appears clear from the interpretation of the UV–vis, EPR, and NMR data, along with comparison of data from other cupredoxins, that the overexpressed protein encoded by the SCO7674 gene of *S. coelicolor* is a cupredoxin.

Co(II)-Substituted Lpc and Metal–Ligand Interplay. For Co(II)-cupredoxins, the δ_{pc} part of the δ_{obs} is, unlike in the native Cu(II) forms, non-negligible. Dissection of the δ_{pc} from the δ_{Fc} can be determined from a prior knowledge of the magnetic susceptibility tensor (χ).⁶⁶ The components and angles of the χ -tensor have been determined for Co(II)-Rc⁶⁷ and Co(II)-Az.⁶⁸ The latter possesses trigonal bipyramidal geometry, and it is assumed that the χ -tensor in tetrahedral Co(II)-cupredoxins with Met as the axial ligand is more similar to Co(II)-Rc.^{61,62} Therefore, the δ_{pc} and δ_{Fc} contributions to the δ_{obs} in Co(II)-Lpc can be assumed to be similar to those in Co(II)-Rc and therefore to those in all other Co(II)-substituted cupredoxins other than Az. Of the Co(II)-cupredoxin NMR spectra reported, Co(II)-Lpc shows the highest similarity to Co(II)-Ami. This may not be entirely surprising, considering the high homology and length of the C-terminal ligand loop and the data from the Cu(II) form of the protein. However, a number of differences between Co(II)-Lpc and Ami are apparent (Table 2).

The most striking difference is in the δ_{obs} values of the Cys C^βH protons, which are separated by 7.9 ppm and are some 60

ppm upfield shifted in comparison to those of Co(II)-Ami (Table 2). On comparing the average shift of these protons, $\delta_{\beta \text{av}}$, for all other reported Co(II)-cupredoxins with Met as the axial ligand, Co(II)-Lpc is the lowest: $\delta_{\beta \text{av}} = 277$ (Pc), 285 (Ami), 291 (pAz), 260 (Rc), and 221 ppm (Lpc). Assuming a χ -tensor similar to that of Rc, then ~30% of the δ_{obs} for these protons in Co(II)-cupredoxins arises from a δ_{pc} contribution, with the remainder from δ_{Fc} . In their Cu(II) counterparts, the δ_{obs} for the corresponding protons is considerably greater. For example, in Cu(II)-Pc, shifts of 650 and 450 ppm,¹⁹ compared to 299 and 275 ppm in Co(II)-Pc, are observed.⁶¹ This is indicative of the Cys C^βH protons in Co(II) proteins possessing much smaller δ_{Fc} , even though Co(II) centers have three unpaired electrons, compared to one in Cu(II) centers. Thus, the Co(II)-Cys bond is much less covalent than that in Cu(II). Despite this, changes in the Cu(II)-Cys interaction are reflected in similar changes in the Co(II)-Cys bonding, scaled down by the reduced covalence of this bond.⁶² Therefore, for Lpc, the Co(II) NMR data are consistent with a decreased spin density onto the Cys ligand, indicative of a longer M(II)-Cys bond than implied for Ami, but also for Pc, pAz, and Rc.

For the Met signals, the δ_{obs} is dominated by large δ_{Fc} values, which are influenced by the Co(II)–S^δ–C^γ–H^γ dihedral angles, whereas the $\delta_{\gamma \text{av}}$ for C^γH protons is not so affected.⁶¹ For Co(II)-Ami, Pc, pAz, and Rc, $\delta_{\gamma \text{av}} = 71.3, 163.2, 188.6,$ and 191.5 ppm, respectively. For Co(II)-Lpc, a $\delta_{\gamma \text{av}}$ of 82.1 ppm is obtained, which is most similar to that of Co(II)-Ami. The lower $\delta_{\gamma \text{av}}$ for Ami has been attributed to the conformation of the Met ligand side chain. In Ami, the torsion angles of the Met side chain result in a gauche configuration at C^α–C^β and C^γ–S^δ, whereas in Pc, pAz, and Rc, a trans conformation is observed.⁶⁹ These structural differences appear to result in different electron delocalization patterns in the axial Met ligand for Co(II)-substituted cupredoxins, but moreover they are indicative of Lpc having a Met ligand side chain with a gauche conformation.

Midpoint Potential of Lpc. At +605 mV, the E° for Lpc is the highest determined for a cupredoxin possessing a “classic” Type-1 copper site. Rc, with a perturbed Type-1 copper site, has a higher E° , +680 mV, but is only stable at acidic pH (<4).⁵⁶ E° for cupredoxins normally range from +185 to +395 mV, with the non-axially ligated, trigonal planar Type-1 copper sites found in multicopper oxidases, such as laccases and ceruloplasmin, having potentials in the 800–1000 mV range.^{70,71} Evidence has been presented that the protein fold constrains the Cu(I) redox state more than the Cu(II) state in low-potential cupredoxins (i.e., Cu(II)/Cu(I) < 400 mV).^{59,72} As the constraint on the Cu(I) redox state is relaxed, the E° increases. This has been clearly demonstrated for Pro mutants in the C-terminal copper-binding loop (–C–(x)_n–P–H–) of Ami and pAz.^{72–74} For Lpc, the absence of a Pro in this segment (Figure 1A) therefore argues for a more flexible region, loosening the

(66) Ubbink, M.; Worrall, J. A. R.; Canters, G. W.; Groenen, E. J. J.; Huber, M. *Annu. Rev. Biophys. Biomol. Struct.* **2002**, *31*, 393–422.

(67) Donaire, A.; Jimenez, B.; Moratal, J. M.; Hall, J. F.; Hasnain, S. S. *Biochemistry* **2001**, *40*, 837–846.

(68) Donaire, A.; Salgado, J.; Moratal, J. M. *Biochemistry* **1998**, *37*, 8659–8673.

(69) Guss, J. M.; Merritt, E. A.; Phizackerley, R. P.; Freeman, H. C. *J. Mol. Biol.* **1996**, *262*, 686–705.

(70) Machonkin, T. E.; Zhang, H. H.; Hedman, B.; Hodgson, K. O.; Solomon, E. I. *Biochemistry* **1998**, *37*, 9570–9578.

(71) Palmer, A. E.; Randall, D. W.; Xu, F.; Solomon, E. I. *J. Am. Chem. Soc.* **1999**, *121*, 7138–7149.

(72) Machczynski, M. C.; Gray, H. B.; Richards, J. H. *J. Inorg. Biochem.* **2002**, *88*, 375–380.

(73) Libeu, C. A. P.; Kukimoto, M.; Nishiyama, M.; Horinouchi, S.; Adman, E. T. *Biochemistry* **1997**, *36*, 13160–13179.

(74) Carrell, C. J.; Sun, D.; Jiang, S.; Davidson, V. L.; Mathews, F. S. *Biochemistry* **2004**, *43*, 9372–9380.

```

Lipocyanin -----MPFPFPTGAARLAAAACALALTALVGCSDGGGGGGGGGATESATRSS-----
Rha07251 -MKRVLTLLVLPILLAVFALAAACGSDGDDSSGSAESAHGDDHPMSGMPMSMSMPMS----
NP_963153 -----MGMTLAKSLTAALAVAVAVAACS---APRPAAGGGTPTSTQTPVTAPP-----
Nfa8770 MPTLHRGLSARVVAALALTASIALAGCGSDASESAPSSSTALTTAPATSAP-----
AAM12874 -MKITLRMMVLAVLTAMAMVLAACGGGGSSGGSTGGGSGSGPVTIEIGSKGEELAF----
CAA82942 --MKDISRRRFVLGTGATVAATLAGCNGNGNGNGNGNGNGEPTPEGRADQFLTDNDAL
CAB84961 -MKAYLALISA AVIGLAACSQEPAPAAEATPAEAPASEAPAAEAPADA AEAP-----

CAC17491 -----ASGGTQVTI-----KDFTFEPASLTVSPGA---KVTVVNKDS-----TTH
Rha07251 --MPAGAGQAGGHEILI-----SDFKYTLPG-TFAPGE---EVTVRNNDT-----AEH
NP_963153 -----AAAGPNQVVI-----DGFAPATLTVPAGT---TVTWINRDE-----EPH
Nfa8770 -----AGPSSVTVTV-----DDMTFSPENITVGVGD---TVTWFSDS-----APH
AAM12874 --DKTELTVSAGQTVTIRF---KNNSAVQQHNIWLVKGGEEAANIANAGLSAG--PAAN
CAA82942 MYDGDITDETQDEVVVVTGAGNNGFAFDPAAIRVDVGT---TVTWEWTDG-----GAH
CAB84961 -----AAGNCAATVESN-----DNMQFNTKDIQVSKACKEFTITLKHGTQPKTSMGHN

CAC17491 TLTASKGGSFDTGDIAPKGSATFTAPS-----TAGDFP
Rha07251 TVTADTGDLFDV-EVEPGATATFTVPG-----QPPTFA
NP_963153 TVAASDG-SFHSPGMGTGAVFTHTF-----AAGTFD
Nfa8770 SVQGIQDKAMGINSPIIDSGEWSYTF-----VPGTFR
AAM12874 YLPADKSNIIAESPLANGNETVEVTFAP-----AAGTYL
CAA82942 NVVSEPESEDFEFESDRVDEEGFTFEQTFD-----DEGVAL
CAB84961 IVIGKTEDMDGIFKDGVGAAADTVYKPPDDARVVAHTKLIGGGEESLTDPAKLADGEYK

CAC17491 YACTIH---PFMKGTLTVE-
Rha07251 FHCAVH---PNMVGTLVLR-
NP_963153 YVCSIH---PMMRGTVVVTVG
Nfa8770 YLCTLH---POMRGSVTVE-
AAM12874 YICTVPGHYPLMOGKLVVN-
CAA82942 YVCTPHR-AQGMYGAVIVE-
CAB84961 FACTFPGHGALMNGKVTLVD

```

Figure 7. Clustal W sequence alignment of putative lipo-cupredoxins: Lpc (SCO7674, CAC17491, *S. coelicolor*), Rha07251 (*Rhodococcus* RHA1), NP_963153 (MAP4219, *Mycobacterium avium*), Nfa8770 (*Nocardia farcina*), CAB84961 (*Neisseria meningitidis*), AAM12874 (Auracyanin, *Chloroflexus aurantiacus*), and CAA82942 (Halocyanin, *Natronomas pharaonis*). The former four strains are all bacteria, and the latter three strains are archaea. Sequences were taken from the protein databases or the genome sequence websites. The Cys residues that are putatively modified by lipid attachment are indicated in bold, with the predicted ligands to the Cu bold and underlined. The following sequences were also found in the databases but were not included in the alignment: Rha03104 (*Rhodococcus* RHA1), CAA29561 (*Neisseria gonorrhoeae*), ZP_00399449 (*Anaeromyxobacter dehalogenans*), NP_634368 (*Methanosarcina mazeri*), NP_616293 (*Methanosarcina acetivorans*), NP_988117 (*Methanococcus maripaludis*), and YP_135135 (*Haloarcula marismortui*).

constraints imposed on the Cu(I) redox state and contributing to the elevated E° . A further consideration is the H-bond networks in the vicinity of the copper site. In nearly all cupredoxin sequences, an Asn residue precedes the N-terminal His ligand. This Asn provides three H-bonds (backbone NH, side-chain amine, and carboxyl group), which “zips” the C-terminal ligand loop to the remainder of the protein. Severing of these H-bonds, as indicated for the N47L variant of Az, results in an increased E° over the native protein.⁷⁵ Significant changes in E° have also been observed for Rc upon mutating a Ser residue found in the analogous position to the Asn.⁷⁶ For Lpc, this residue is Thr58, which from the Cu(II) NMR data is indicated to maintain the (Thr58)–H^N–S–(Cys93) H-bond. However, it is the side-chain H-bonding interactions which appear to exert the controlling influence on the copper ion E° . This leads us to propose that the fact that Thr58 in Lpc has one less functional group to offer to actively participate in a H-bond interaction also contributes to the elevated potential.

Alkaline and Acid Transitions. At alkaline pH, a deprotonation event perturbs the electronic properties of the Cu(II) active site for members of the phytocyanins and the bacterial pAz.^{77,78} Upon increasing the pH, the LMCT bands in the UV-vis spectrum of Cu(II)-Lpc shift toward the blue, and a pK_a of

~10 is obtained. This coincides with the reported pK_a 's of 9–11 for this alkaline transition. It is noted, however, that the LMCT bands in the Lpc spectrum do not exhibit as large a shift as observed for phytocyanins or pAz.^{77,78} A conserved Lys residue adjacent to the axial Met ligand is present in all species which exhibit an alkaline transition, and it has been suggested that deprotonation of this residue triggers the transition.⁷⁷ This Lys is also present in Lpc (Figure 1A). However, mutagenesis of this Lys in umecyanin did not lead to the expected abolition of the alkaline transition, and more complicated factors are seemingly involved.⁷⁹ Nevertheless, regardless of the cause or the physiological significance of this transition in vivo, Lpc is another bacterial cupredoxin which in vitro undergoes an alkaline transition.

For all Pc's (except *Dryopteris crassirhizoma*⁸⁰), Ami, and pAz, an active-site protonation of the N-terminal His ligand in the Cu(I) state is observed, with pK_a 's ranging between 7.0 and 4.8.^{72,81–83} For Lpc, no protonation is apparent, and therefore it belongs with the cupredoxins Az, Rc, and auracyanin (Au), for which no active-site His protonation is observed. Recent studies have challenged the many hypotheses put forward to try and explain why some cupredoxins exhibit an acid transition

(75) Hoitink, C. W. G.; Canters, G. W. J. *Biol. Chem.* **1992**, *267*, 13836–13842.

(76) Hall, J. F.; Kanbi, L. D.; Harvey, I.; Murphy, L. M.; Hasnain, S. S. *Biochemistry* **1998**, *37*, 11451–11458.

(77) Dennison, C.; Harrison, M. D.; Lawler, A. T. *Biochem. J.* **2003**, *371*, 377–383.

(78) Kohzuma, T.; Dennison, C.; Mcfarlane, W.; Nakashima, S.; Kitagawa, T.; Inoue, T.; Kai, Y.; Nishio, N.; Shidara, S.; Suzuki, S.; Sykes, A. G. J. *Biol. Chem.* **1995**, *270*, 25733–25738.

(79) Harrison, M. D.; Yanagisawa, S.; Dennison, C. *Biochemistry* **2005**, *44*, 3056–3064.

(80) Kohzuma, T.; Inoue, T.; Yoshizaki, F.; Sasakawa, Y.; Onodera, K.; Nagatomo, S.; Kitagawa, T.; Uzawa, S.; Isobe, Y.; Sugimura, Y.; Gotowda, M.; Kai, Y. *J. Biol. Chem.* **1999**, *274*, 11817–11823.

(81) Dennison, C.; Kohzuma, T.; Mcfarlane, W.; Suzuki, S.; Sykes, A. G. J. *Chem. Soc., Chem. Commun.* **1994**, 581–582.

(82) Lommen, A.; Canters, G. W.; Vanbeeumen, J. *Eur. J. Biochem.* **1988**, *176*, 213–223.

(83) Segal, M. G.; Sykes, A. G. *J. Am. Chem. Soc.* **1978**, *100*, 4585–4592.

and others do not.⁵⁴ These have led to the suggestion that, in principle, all Cu(I) cupredoxins have an acid transition, but in certain cases the protonation and dissociation of the C-terminal His ligand require such a low pH that the protein is no longer stable enough for it to be observed experimentally.⁸⁴ Therefore, for Cu(I)-Lpc, the small upward increase in midpoint potential at the end of the accessible pH range studied in this work could be considered as the onset of His96 protonation, with a $pK_a \ll 4$, although the protonation of a nearby acidic residue cannot be excluded as a possible cause.

Function of Lpc. From BLAST searches and browsing the various genome sequencing projects, a number of lipo-cupredoxins with a lipoprotein processing sequence in the signal peptide were identified (Figure 7). Therefore, a lipo-cupredoxin as in *S. coelicolor* is not unique, but a high-potential copper site is, compared to the lipo-cupredoxins from archaea in Figure 7.^{85–88} From the sequences of the actinomycetales order in Figure 7, a putative high-potential Type-1 copper site is also inferred, with all sequences lacking a Pro residue in the C–X₂–H segment of the copper-binding motif and a side-chain for the residue after the potential N-terminal His ligand lacking potential H-bonding interactions, as discussed.

The gene organization as depicted in Figure 1B is unique to Lpc, and as far as can be deduced from the genome sequences of the other species (some are not yet finished), the environment surrounding the lipo-cupredoxin gene in each species presented in Figure 7 is different. This makes it difficult, at present, to infer a function for these high-potential lipo-cupredoxins.

However, it is generally accepted that genes organized on a genome, as in the present case, may be functionally related. The gene organization does suggest that Lpc is located in the membrane in complex or together with the upstream and downstream encoded proteins (a lipoprotein and membrane protein) (Figure 1B). Furthermore, immediately downstream of this operon and transcribed in the same direction, genes are present encoding a ferredoxin and a solute-binding-protein-dependent ABC transporter. Since lipoproteins such as Lpc are supposed to be located on the outside of the cell in Gram-positive bacteria, a substrate for Lpc is likely to come from this environment. We therefore speculate that this substrate undergoes reduction/oxidation by Lpc before uptake by the ABC transporter, followed by reduction/oxidation by the ferredoxin once inside. As *S. coelicolor* is a soil-dwelling organism, location of the Lpc on the outside of the bacterial envelope entails an oxidizing environment for the Lpc to operate in. Ferredoxins cover a broad range of midpoint potentials, the high end of which, however, is still well below the Lpc midpoint potential. If the ferredoxin and the Lpc operate in tandem in redox-coupled membrane transport, the logical sequence would be oxidation of the substrate by the Lpc and reduction back by the ferredoxin. Back oxidation of the Lpc by oxygen might be mediated through an extracellular oxidase, for instance, of which a few have been identified already on the *S. coelicolor* genome. Membrane transport would be coupled, thus, to anti-transport electron flow. Morphological studies with an *lpc* knockout mutant of *S. lividans* may give more information about the physiological role of Lpc.

Acknowledgment. This work was supported by the Netherlands organization for scientific research, grant no. 98S1010.

Supporting Information Available: Complete ref 15. This material is available free of charge via the Internet at <http://pubs.acs.org>.

JA064112N

- (84) Dennison, C.; Lawler, A. T.; Kohzuma, T. *Biochemistry* **2002**, *41*, 552–560.
(85) Gotschlich, E. C.; Seiff, M. E. *FEMS Microbiol. Lett.* **1987**, *43*, 253–255.
(86) Mattar, S.; Scharf, B.; Kent, S. B. H.; Rodewald, K.; Oesterhelt, D.; Engelhard, M. *J. Biol. Chem.* **1994**, *269*, 14939–14945.
(87) Rooney, M. B.; Honeychurch, M. J.; Selvaraj, F. M.; Blankenship, R. E.; Bond, A. M.; Freeman, H. C. *J. Biol. Inorg. Chem.* **2003**, *8*, 306–317.
(88) Brischwein, M.; Scharf, B.; Engelhard, M.; Mantele, W. *Biochemistry* **1993**, *32*, 13710–13717.
(89) Schaerlaekens, K.; Van Mellaert, L.; Lammertyn, E.; Geukens, N.; Anne, J. *Microbiology-Sgm* **2004**, *150*, 21–31.